

NEUROSCIENCE

Microglia mediate forgetting via complement-dependent synaptic elimination

Chao Wang^{1,2,*}, Huimin Yue^{1,2,*}, Zhechun Hu^{1,2}, Yuwen Shen^{1,2}, Jiao Ma³, Jie Li^{1,2}, Xiao-Dong Wang^{4,5}, Liang Wang⁶, Binggui Sun⁷, Peng Shi⁸, Lang Wang^{3,†}, Yan Gu^{1,2,9,†}

Synapses between engram cells are believed to be substrates for memory storage, and the weakening or loss of these synapses leads to the forgetting of related memories. We found engulfment of synaptic components by microglia in the hippocampi of healthy adult mice. Depletion of microglia or inhibition of microglial phagocytosis prevented forgetting and the dissociation of engram cells. By introducing CD55 to inhibit complement pathways, specifically in engram cells, we further demonstrated that microglia regulated forgetting in a complement- and activity-dependent manner. Additionally, microglia were involved in both neurogenesis-related and neurogenesis-unrelated memory degradation. Together, our findings revealed complement-dependent synapse elimination by microglia as a mechanism underlying the forgetting of remote memories.

Memory is coded and allocated to engrams within related brain regions (1, 2). Reactivation of engram cells is essential for memory recall, whereas failure in reactivation of engram cells leads to the forgetting of related memories (3). Synaptic connections between engram cells are believed to be substrates for memory storage (4, 5). Circuit rewiring and synaptic reorganization may lead to loss or weakening of synaptic connections between engram cells, resulting in the forgetting of previously existing memories. For example, massive synaptic reorganization takes place in the dentate gyrus (DG) as continuously generated newborn neurons integrate into the hippocampal neural circuit, which leads to the forgetting of hippocampus-dependent memories (6–8). Even in mature neurons, experience- and learning-dependent, dynamic remodeling of synapses occurs con-

stantly throughout life (9–13), providing a potential mechanism for the erasure of stored memories in the synaptic connections of these cells. Microglia are not only important for pruning excessive synapses during postnatal brain development but are also involved in the dynamics of synapses in the adult brain (14–17). Because they survey the brain and play crucial roles in monitoring synapses and determining the wiring of the brain (15, 18, 19), microglia may affect the stability of synaptic connections within the neural circuits where memories are allocated.

First, we used contextual fear conditioning (CFC) to assess the memory retention in C57BL/6 mice. We measured the freezing behavior of the animals during a test performed 5 or 35 days after three training sessions, each training session consisting of three weak foot shocks (Fig. 1A). We observed a significant decrease in the freezing of animals at 35 days compared with 5 days after training (Fig. 1B). We then carried out CFC training using CD11b-DTR mice, in which diphtheria toxin receptor (DTR) is specifically expressed in CD11b-expressing myeloid cells, including microglia in the brain (20). By intracerebroventricularly administering diphtheria toxin (DT) daily after training, we depleted microglia in these CD11b-DTR mice until the test (fig. S1). Thirty-five days later, CD11b-DTR mice treated with DT showed significantly higher freezing levels than those in the saline group (fig. S1). To avoid the effect of daily injection on animal behaviors, we depleted microglia in C57BL/6 mice with PLX3397 (PLX), a CSF1R/c-kit antagonist (21), via mouse diet after CFC training (Fig. 1C). Thirty-five days later, PLX treatment significantly increased freezing of the animals (Fig. 1D), with microglia depleted in the brain (Fig. 1, E and F), consistent with the results obtained from CD11b-DTR mice.

To exclude the possibility that depleting microglia may affect formation or retrieval

of memories, we tested the freezing of mice a short time (5 days) after training (fig. S2A). We found that PLX treatment did not alter the freezing of animals (fig. S2B). Furthermore, we started administration of PLX to deplete microglia before the training and tested 24 hours later (fig. S2C). No significant difference was observed between control and PLX-treated animals (fig. S2D). Further behavioral tests showed that PLX treatment for 35 days did not significantly change the behavior of animals in an elevated plus maze or an open field (fig. S3).

Memory retrieval requires reactivation of engram cells (3), whereas dissociation of engram cells—i.e., engram cells being unable to reactivate at the same time—leads to forgetting. To test whether the microglia-mediated forgetting of already-formed memory correlates with dissociation of engram cells, we used a FosTRAP strategy for tagging activated neurons during CFC training (22). We trained c-Fos-Cre^{ERT2}::Ai14 mice for contextual fear memory and administered tamoxifen (TAM) before the last training session to induce permanent expression of dTomato in activated engram neurons. Immunofluorescent staining for c-Fos was performed after the test, and the reactivation rate of engram cells was assessed by analyzing c-Fos⁺dTomato⁺ colocalization in the DG (Fig. 1, G and H). Under physiological conditions, the reactivation rate of engram cells 35 days after training significantly decreased compared with that measured at 5 days, which correlates with the forgetting of related memory (Fig. 1I). Thirty-five days but not 5 days after training, PLX treatment significantly increased the reactivation rate of the engram cells (Fig. 1I), without altering the number of dTomato⁺ engram cells in the DG (fig. S4). The freezing of animals during the test positively correlates with the reactivation rate of engram cells (Fig. 1J).

During postnatal development, microglia are involved in synaptic reorganization and circuitry refinement by synaptic pruning (15). We imaged microglia in the DG of adult CX3CR1^{GFP/+} mice, in which microglia were labeled with green fluorescent protein (GFP). When costained with synaptophysin or PSD95, markers for pre- or postsynaptic components, we found synaptophysin⁺ and PSD95⁺ puncta were present in GFP⁺ microglia, colocalizing with lysosome marker Lamp1 (Fig. 2, A and B, and movies S1 and S2).

To test whether synaptic elimination by microglial phagocytosis may mediate forgetting, we systematically administered minocycline (Mino)—which has been shown to inhibit microglial engulfment of synapses in vitro and in vivo (15, 23)—after CFC training until the test (fig. S5A). Thirty-five days later, Mino-treated animals showed significantly longer freezing time (fig. S5B). Immunostaining showed that microglia in Mino-treated CX3CR1^{GFP/+} animals

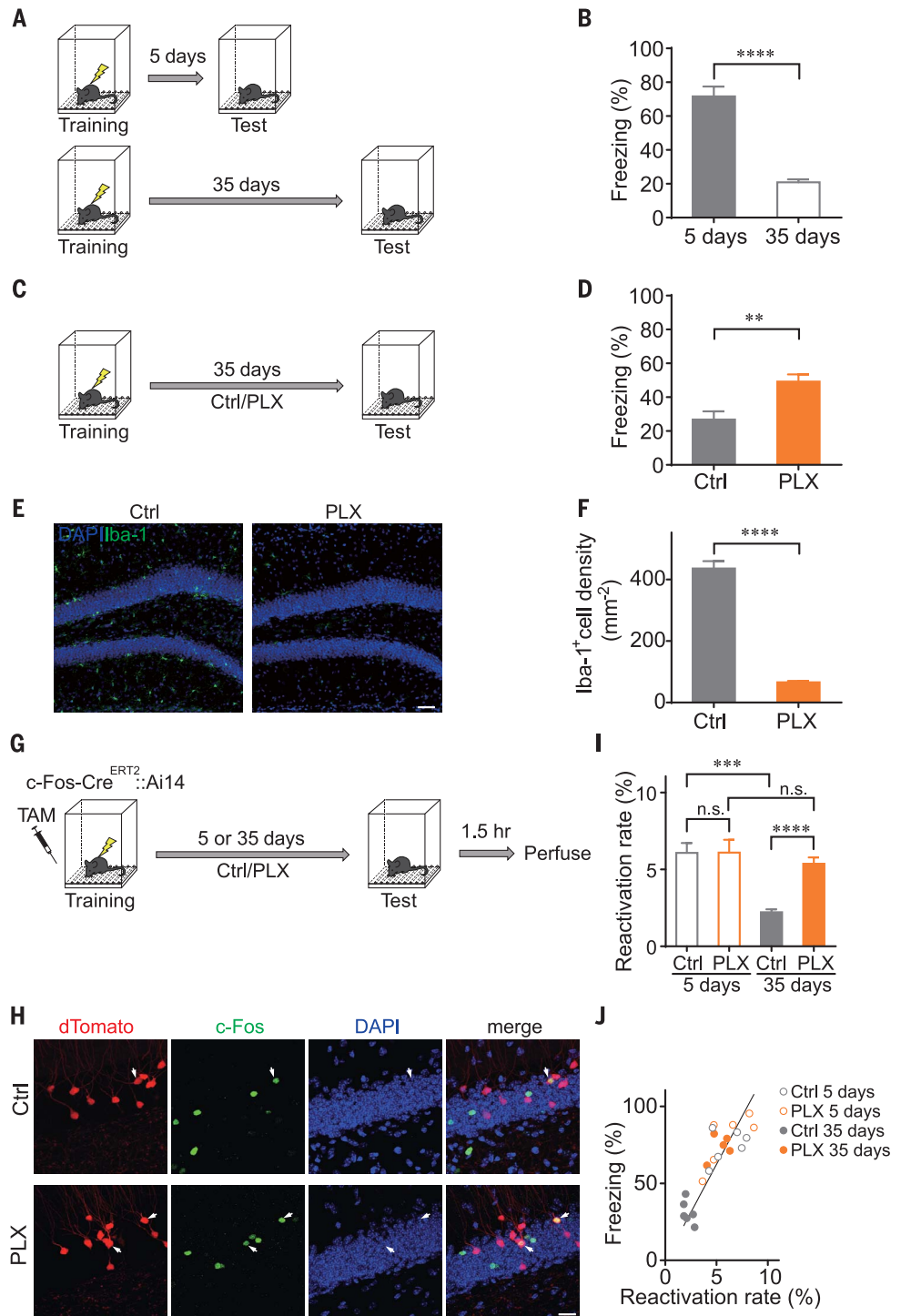
¹Institute of Neuroscience and Department of Neurology of the Second Affiliated Hospital, NHC and CAMS Key Laboratory of Medical Neurobiology, Zhejiang University School of Medicine, Hangzhou 310058, China. ²Center for Stem Cell and Regenerative Medicine, Zhejiang University School of Medicine, Hangzhou 310058, China. ³Department of Neurology of the First Affiliated Hospital, Interdisciplinary Institute of Neuroscience and Technology, Zhejiang University School of Medicine, Hangzhou 310029, China. ⁴Department of Neurobiology, Institute of Neuroscience, NHC and CAMS Key Laboratory of Medical Neurobiology, Zhejiang University School of Medicine, Hangzhou 310058, China. ⁵Department of Psychiatry, Sir Run Run Shaw Hospital, Zhejiang University School of Medicine, Hangzhou 310016, China. ⁶Institute of Neuroscience and Department of Neurology of the Second Affiliated Hospital, Mental Health Center, NHC and CAMS Key Laboratory of Medical Neurobiology, Zhejiang University School of Medicine, Hangzhou 310058, China. ⁷Center for Neuroscience and Department of Neurology of the First Affiliated Hospital, NHC and CAMS Key Laboratory of Medical Neurobiology, Zhejiang University School of Medicine, Hangzhou 310058, China. ⁸Department of Cardiology of the Second Affiliated Hospital, Zhejiang University School of Medicine, Hangzhou 310058, China. ⁹Zhejiang Provincial Key Laboratory of Tissue Engineering and Regenerative Medicine, Hangzhou 310058, China.

*These authors contributed equally to this work.

†Corresponding author. Email: wanglang@zju.edu.cn (L.W.); guyan2015@zju.edu.cn (Y.G.)

Fig. 1. Depletion of microglia prevents memory forgetting and engram dissociation.

(A) Adult mice received CFC training and were tested 5 or 35 days later. **(B)** Animals showed significantly reduced freezing 35 days after training compared with 5 days after training. $n = 9$ mice per group; $t = 8.316$, $df = 16$; **** $P < 0.0001$. Error bars indicate standard error of the mean (SEM). **(C)** After CFC training, mice received normal food [control (Ctrl)] or food containing PLX before the test 35 days after training. **(D)** PLX treatment decreased forgetting. Ctrl $n = 19$ mice, PLX $n = 17$ mice; $t = 3.443$, $df = 34$, ** $P = 0.0015$. **(E)** Confocal images showing decreased number of microglia (Iba1⁺) in the DG of PLX-treated animals. Scale bar, 50 μm ; DAPI, 4',6-diamidino-2-phenylindole. **(F)** PLX significantly decreased the density of microglia in the DG. Ctrl $n = 4$ mice, PLX $n = 7$ mice; $t = 20.39$, $df = 9$, **** $P < 0.0001$. **(G)** c-Fos-Cre^{ERT2}::Ai14 mice were treated with TAM before the last training and then received Ctrl or PLX food until the test 5 or 35 days after training. **(H)** Confocal images showing the reactivation of engram cells in the DG of c-Fos-Cre^{ERT2}::Ai14 mice. White arrows indicate reactivated engram cells (c-Fos⁺dTomato⁺) during test. Scale bar, 20 μm . **(I)** Reactivation rate of engram cells (c-Fos⁺dTomato⁺/dTomato⁺) decreased from 5 days to 35 days after training (Ctrl 5 days, $n = 6$ mice, versus Ctrl 35 days, $n = 6$ mice, $t = 5.750$, $df = 10$, *** $P = 0.0002$), whereas PLX3397 treatment prevented the decrease of reactivation rate over time (PLX 5 days, $n = 6$ mice, versus PLX 35 days, $n = 5$ mice, $t = 0.7272$, $df = 9$, $P = 0.4856$). PLX3397 treatment increased the reactivation rate of engram cells 35 days after training (Ctrl 35 days versus PLX 35 days, $t = 7.340$, $df = 9$, **** $P < 0.0001$), but not 5 days (Ctrl 5 days versus PLX 5 days, $t = 0.01618$, $df = 10$, $P = 0.9874$). n.s., not significant. **(J)** The reactivation rate of DG engram cells is positively correlated with freezing of animals. Ctrl 5 days, gray open circles, $n = 6$ mice; PLX 5 days, orange open circles, $n = 6$ mice; Ctrl 35 days, gray solid circles, $n = 6$ mice; PLX 35 days, orange solid circles, $n = 5$ mice. Solid line indicates linear fitting of all points; $R^2 = 0.5998$, where R^2 is the coefficient of determination.



contained smaller synaptophysin⁺ puncta (fig. S5, C and D) or PSD95⁺ puncta (fig. S5, E and F).

Complement cascades are important for tagging synapses to be eliminated by microglia during brain development. C1q, the initiating protein of the classical complement cascade, localizes to synapses during developmental circuit refinement (24). C1q-tagging of the synapses leads to deposition of C3, which activates C3 receptors on microglia and triggers

synaptic elimination by microglial phagocytosis (15, 24). We found that C1q was present within microglia, colocalizing with PSD95 and CD68, a microglial lysosomal marker (Fig. 2C and movie S3). Furthermore, using brain sections from c-Fos-Cre^{ERT2}::Ai14 mice, in which engram cells were labeled with dTomato, we found colocalization of C1q with $\sim 1.193 \pm 0.335\%$ of the dendritic spines of engram cells (Fig. 2, D and E, and movie S4) as well as colocalization

of dTomato, PSD95, and CD68 within microglia (Fig. 2F and movie. S5). Correspondingly, engram cells showed higher spine density in PLX-treated animals (fig. S6).

To test whether complement pathways are responsible for microglia-mediated engram dissociation and forgetting, we constructed a Cre-dependent adeno-associated virus (AAV) vector expressing CD55 (also known as decay-accelerating factor, or DAF), which is a

Fig. 2. Microglia mediate forgetting through complement system.

(A and B) Superresolution microscopy images and three-dimensional (3D) reconstructions showing the presence of synaptophysin (Syn) or PSD95 in microglia (GFP⁺), colocalizing with Lamp1, in the DG of CX3CR1^{GFP/+} mice. Scale bars, 5 μ m; white arrows indicate Syn⁺Lamp1⁺ (A) or PSD95⁺Lamp1⁺ (B) puncta within microglia. **(C)** Images and 3D reconstruction showing the presence of C1q and PSD95 in microglia, colocalizing with CD68. Scale bars, 5 μ m; white arrows indicate PSD95⁺CD68⁺C1q⁺ puncta within microglia. **(D)** Images and 3D reconstruction showing colocalization of C1q with a dendritic spine of an engram cell (dTomato⁺) in the DG. Scale bars, 1 μ m; white arrows indicate colocalization of C1q with a dendritic spine of an engram cell. **(E)** Percentage of engram cell dendritic spines showing colocalization with C1q. $n = 3$ mice, $N = 76$ dendritic segments. **(F)** Images and 3D reconstruction showing the presence of engram cell components (dTomato⁺) in the microglia (Iba-1⁺), colocalizing with PSD95 and CD68. Scale bars, 5 μ m; white arrows indicate dTomato⁺CD68⁺PSD95⁺ puncta within microglia. **(G)** Diagram of AAV vectors.

(H) Experimental scheme for expressing CD55 in engram cells in the DG of c-Fos-Cre^{ERT2} mice. **(I)** CD55 animals showed higher freezing level. mCherry $n = 21$ mice, CD55 $n = 17$ mice; $t = 5.033$, $df = 36$, **** $P < 0.0001$. **(J)** Images showing engram cells labeled by mCherry or CD55 AAV vectors (red) in the DG and neurons activated during the test expressed by c-Fos (green). White arrows indicate reactivated engram cells (mCherry⁺c-Fos⁺). Insets show the colocalization of mCherry and c-Fos. Scale bar, 20 μ m. **(K)** Reactivation rate of engram cells (c-Fos⁺mCherry⁺/mCherry⁺) showed an increase in CD55 animals. $n = 8$ mice, CD55 $n = 9$ mice; $t = 5.916$, $df = 15$, **** $P < 0.0001$. **(L)** Images showing engram cell components (mCherry⁺) colocalizing with CD68 in microglia (Iba-1⁺) in mCherry mice, but not in CD55 animals. White arrows indicate mCherry⁺/CD68⁺ puncta in microglia. Scale bars, 5 μ m; white arrows indicate mCherry⁺CD68⁺ (mCherry) puncta or mCherry⁺CD68⁺ (CD55) puncta in microglia. **(M)** Percentage of microglia containing mCherry⁺ puncta decreased in CD55 mice. mCherry $n = 3$ mice, $N = 36$ cells; CD55 $n = 4$ mice, $N = 34$ cells; $t = 24.16$, $df = 5$, **** $P < 0.0001$. **(N)** CD55 expression in engram cells decreased the volume of mCherry⁺ puncta in microglia containing mCherry⁺ signals. mCherry $n = 3$ mice, $N = 34$ cells; CD55 $n = 4$ mice, $N = 9$ cells; $t = 3.755$, $df = 41$, *** $P = 0.0005$.

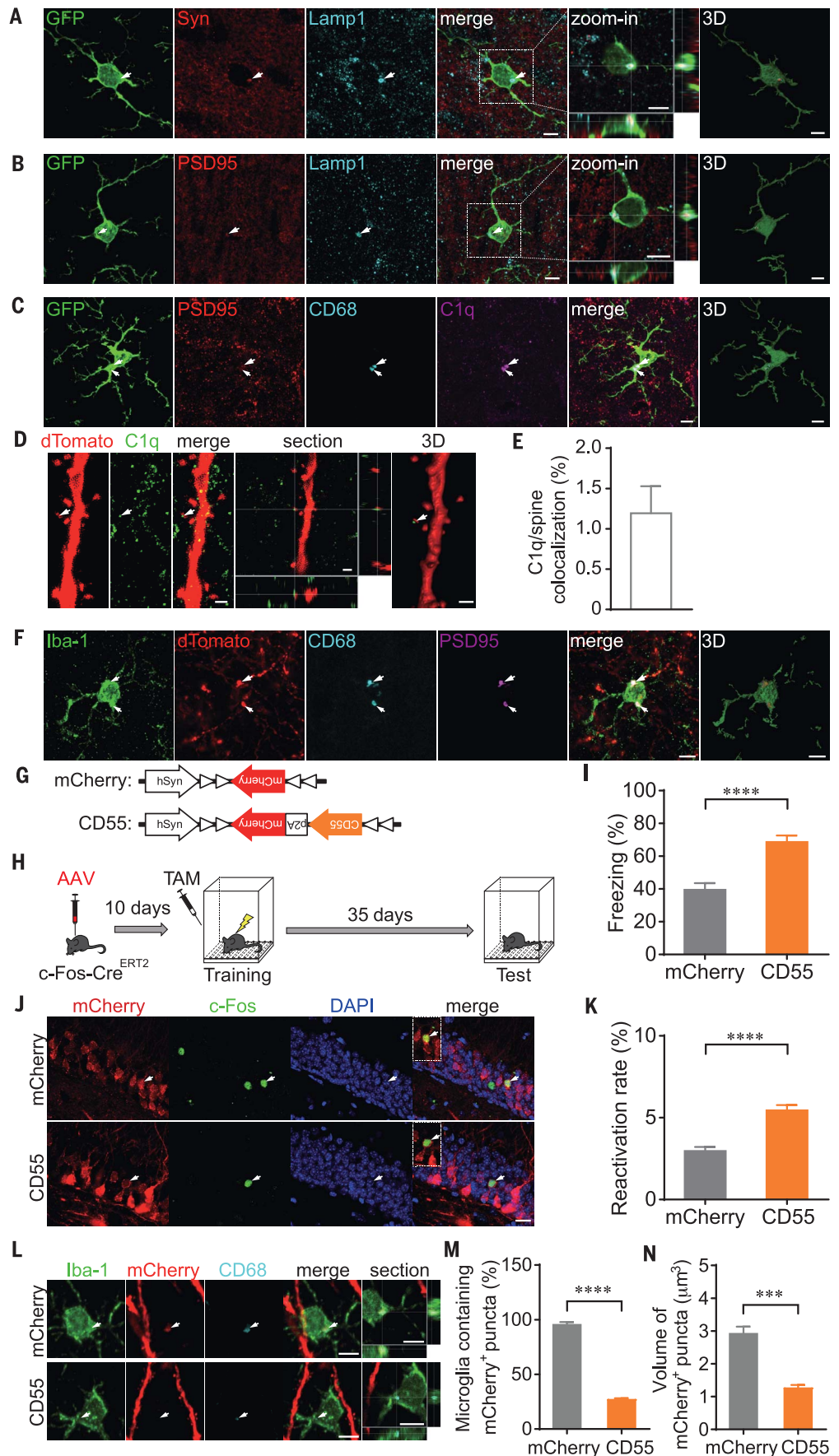


Fig. 3. Microglia mediate forgetting and dissociation of engram cells in an activity-dependent manner. (A) TAM

was administered to c-Fos-Cre^{ERT2}::hM4Di mice before the last training. After training, animals were given food containing PLX and received daily injection of CNO or vehicle (Veh). (B) Freezing of animals during the test 35 days after training. CNO⁻PLX⁻ *n* = 10 mice, CNO⁺PLX⁻ *n* = 8 mice, CNO⁻PLX⁺ *n* = 7 mice, CNO⁺PLX⁺ *n* = 10 mice; CNO⁻PLX⁻ versus CNO⁺PLX⁻ *t* = 3.571, *df* = 16, ***P* = 0.0026; CNO⁻PLX⁻ versus CNO⁻PLX⁺ *t* = 5.068, *df* = 15, ****P* = 0.0001; CNO⁻PLX⁻ versus CNO⁺PLX⁺ *t* = 7.649, *df* = 16, *****P* < 0.0001; CNO⁻PLX⁺ versus CNO⁺PLX⁺ *t* = 0.4716, *df* = 15, *P* = 0.6440. (C) 10 days before CFC training, AAV vectors (mCherry: AAV-hSyn-DIO-mCherry; CD55: AAV-hSyn-DIO-CD55-p2A-mCherry) were injected into the DG of c-Fos-Cre^{ERT2}::hM4Di mice, and TAM was administered to the animals before the last training. After training, animals received injection of CNO or Veh every other day.

(D) Freezing of animals during the test 35 days later. CNO⁻mCherry *n* = 9 mice, CNO⁺mCherry *n* = 12 mice, CNO⁻CD55 *n* = 10 mice, CNO⁺CD55 *n* = 12 mice; CNO⁻mCherry versus CNO⁺mCherry *t* = 3.035, *df* = 19, ***P* = 0.0068; CNO⁻mCherry versus CNO⁻CD55 *t* = 4.843, *df* = 17, ****P* = 0.0002; CNO⁺mCherry versus CNO⁺CD55 *t* = 8.823, *df* = 22, *****P* < 0.0001; CNO⁻CD55 versus CNO⁺CD55 *t* = 0.1057, *df* = 20, *P* = 0.9169. (E) Confocal images showing reactivated (c-Fos⁺) engram cells (mCherry⁺) in the DG during test. White arrows indicate an mCherry⁺c-Fos⁺ cell. Scale bar, 20 μm; white arrows

indicate a reactivated engram cell in the DG (mCherry⁺c-Fos⁺). (F) CNO treatment decreased the reactivation rate of engram cells. (CNO⁻mCherry *n* = 4 mice, CNO⁺mCherry *n* = 4 mice, CNO⁻CD55 *n* = 5 mice; CNO⁻mCherry versus CNO⁺mCherry *t* = 2.937, *df* = 6, **P* = 0.0260), whereas expression of CD55 in engram cells prevented the decrease of reactivation rate (CNO⁻mCherry versus CNO⁺CD55 *t* = 2.895, *df* = 6, **P* = 0.0275; CNO⁺mCherry versus CNO⁺CD55 *t* = 2.435, *df* = 7, **P* = 0.0451; CNO⁻CD55 versus CNO⁺CD55 *t* = 0.4375, *df* = 7, *P* = 0.6749).

known inhibitor of both classical and alternative complement pathways (25). We injected AAV-hSyn-DIO-CD55-p2A-mCherry (CD55) or AAV-hSyn-DIO-mCherry (mCherry) viruses into the DG of c-Fos-Cre^{ERT2} mice 10 days before CFC training, and TAM was administered before the last training to induce the expression of CD55 or mCherry only in DG engram neurons (Fig. 2, G and H, and fig. S7). Thirty-five days after training, mice in the CD55 group showed higher freezing (Fig. 2I) and a higher reactivation rate of engram cells (Fig. 2, J and K). Post hoc staining showed significantly fewer microglia containing mCherry⁺ puncta (Fig. 2, L and M) and smaller mCherry⁺ puncta within Iba-1⁺ microglia in the CD55 group of animals (Fig. 2N).

Connectivity between engram cells is essential for memories (26), whereas microglia-dependent synaptic elimination preferentially targets weak or less-active synapses (15). We next examined whether microglia-mediated forgetting depends

on the activity of engram neurons. We trained c-Fos-Cre^{ERT2}::hM4Di mice for contextual fear memory and administered TAM to induce the expression of inhibitory DREADD (designer receptors exclusively activated by designer drugs) receptor hM4Di in tagged engram cells. DREADD ligand clozapine-*N*-oxide (CNO) was administered every other day after CFC training to repetitively suppress the activity of tagged engram cells (Fig. 3A). Thirty-five days later, the animals treated with CNO alone exhibited significantly decreased freezing (Fig. 3B), whereas administration of PLX after training prevented the facilitated forgetting in CNO-treated animals (Fig. 3B).

To confirm this result, we injected AAV-hSyn-DIO-CD55-mCherry or AAV-hSyn-DIO-mCherry into the DG of c-Fos-Cre^{ERT2}::hM4Di mice and trained them for conditioned contextual fear memory. TAM was administered to express both hM4Di and CD55/mCherry in

the engram cells (Fig. 3C). The animals treated with CNO alone showed reduced freezing (Fig. 3D) and decreased reactivation rate of labeled engram cells (Fig. 3, E and F). Expression of CD55 prevented the accelerated forgetting (Fig. 3D) and the decreased reactivation rate of engram cells induced by CNO-mediated DREADD inhibition of these cells (Fig. 3F).

In the hippocampal DG, newborn neurons are continuously generated and integrate into the hippocampal neural circuits. This leads to drastic synaptic reorganization and circuit rewiring (7, 27, 28) and the forgetting of hippocampus-dependent memories, especially during infancy when massive neurogenesis is occurring within the DG (6). To investigate the relationship between microglia-mediated memory loss and neurogenesis-mediated forgetting, we enhanced neurogenesis in the DG of CX3CR1^{GFP/+} mice by treating them with memantine (MEM), a pro-neurogenic drug

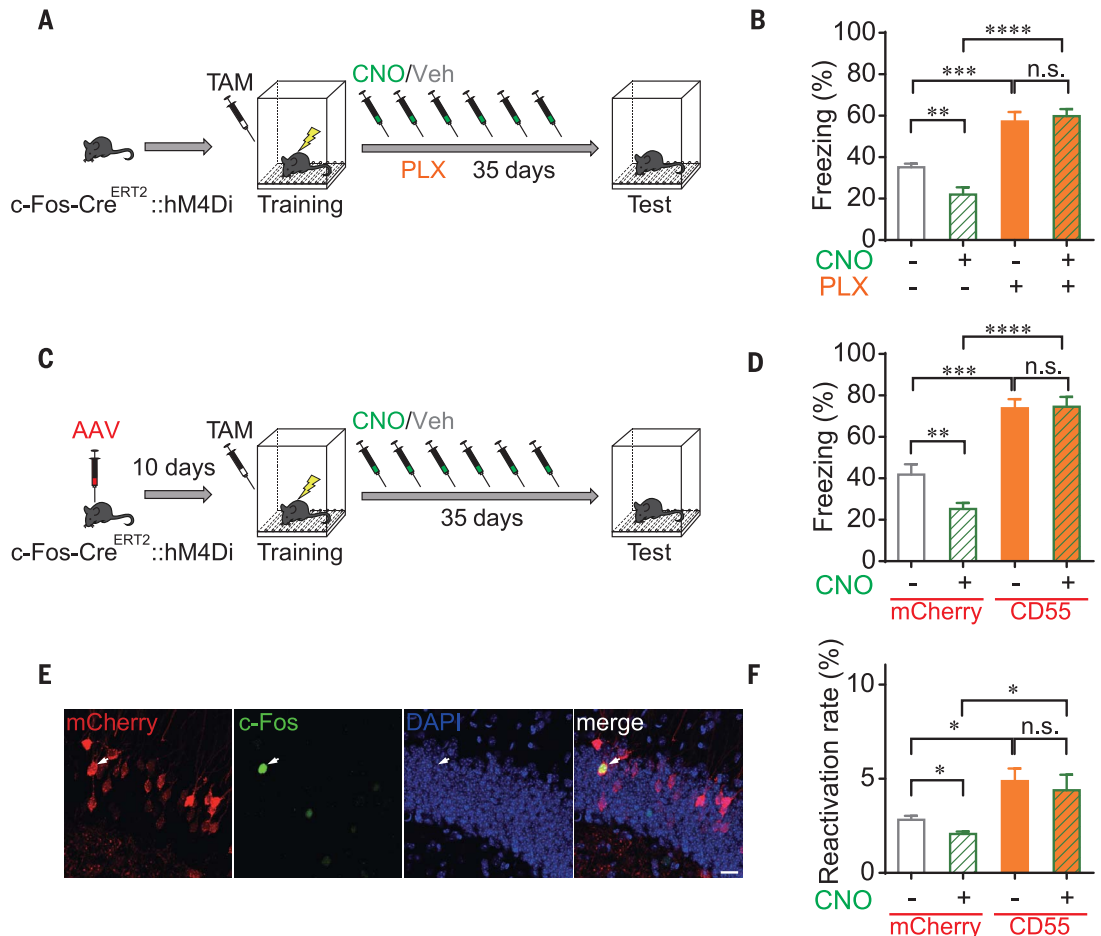
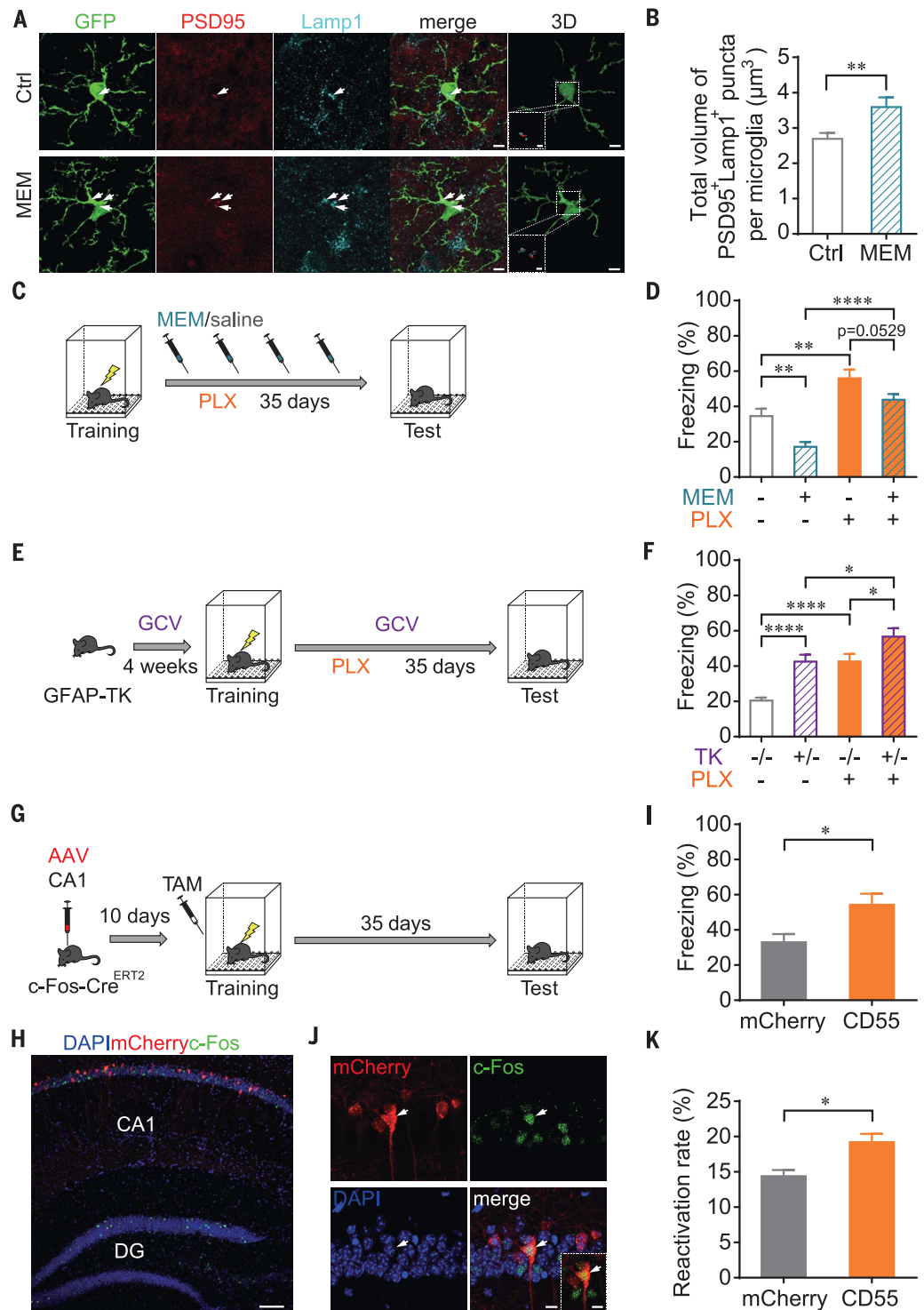


Fig. 4. Microglia contribute to both neurogenesis-mediated and non-neurogenesis-mediated forgetting.

(A) Superresolution images and 3D reconstruction showing the PSD95⁺Lamp1⁺ puncta in microglia in Ctrl and MEM-treated CX3CR1^{GFP/+} mice. Scale bars, 5 μ m; white arrows indicate PSD95⁺Lamp1⁺ puncta in microglia. Insets are enlarged 3D reconstructions of PSD95⁺Lamp1⁺ puncta in microglia. Scale bars, 2 μ m. **(B)** MEM-treatment increased the volume of PSD95⁺Lamp1⁺ puncta in each microglia. Ctrl $n = 3$ mice, $N = 29$ cells; MEM $n = 3$ mice, $N = 30$ cells; $t = 2.774$, $df = 57$, $**P = 0.0075$. **(C)** PLX and MEM treatment administered to mice.

(D) Freezing of animals during the test 35 days after training. MEM⁻PLX⁻ $n = 10$ mice, versus MEM⁺PLX⁻ $n = 10$ mice, $t = 3.511$, $df = 18$, $**P = 0.0025$; MEM⁻PLX⁻ versus MEM⁻PLX⁺ $n = 10$ mice, $t = 3.341$, $df = 18$, $**P = 0.0036$; MEM⁺PLX⁻ versus MEM⁺PLX⁺ $n = 10$ mice, $t = 6.277$, $df = 18$, $****P < 0.0001$; MEM⁻PLX⁺ versus MEM⁺PLX⁺ $t = 2.072$, $df = 18$, $P = 0.0529$. **(E)** GCV and PLX treatment administered to GFAP-TK^{+/-} or GFAP-TK^{-/-} mice. **(F)** Freezing during the test 35 days after training. TK^{-/-}PLX⁻ $n = 14$ mice versus TK^{+/-}PLX⁻ $n = 14$ mice, $t = 5.181$, $df = 26$, $****P < 0.0001$; TK^{-/-}PLX⁻ versus TK^{-/-}PLX⁺ $n = 14$ mice, $t = 4.895$, $df = 26$, $****P < 0.0001$; TK^{+/-}PLX⁻ versus TK^{+/-}PLX⁺ $n = 13$ mice, $t = 2.333$, $df = 25$, $*P = 0.0280$; TK^{-/-}PLX⁺ versus TK^{+/-}PLX⁺ $t = 2.2426$, $df = 25$, $*P = 0.0341$. **(G)** c-Fos-Cre^{ERT2} mice received AAV injection into CA1 and recovered for 10 days before CFC training. TAM was administered before the last training, and freezing was tested 35 days later. **(H)** Confocal image showing engram cells (mCherry⁺) in CA1 but not in the DG. Scale bar, 100 μ m. **(I)** CD55 animals showed higher freezing level. mCherry $n = 11$ mice, CD55 $n = 11$ mice; $t = 2.728$, $df = 20$, $*P = 0.0130$. **(J)** Confocal images showing the reactivation of engram cells in CA1. White arrows indicate a reactivated engram cell (mCherry⁺c-Fos⁺) in CA1. Inset shows the colocalization of mCherry and c-Fos; Scale bars, 20 μ m. **(K)** Reactivation rate of engram cells in CA1 was increased in CD55 animals. mCherry $n = 5$ mice, CD55 $n = 5$ mice; $t = 3.268$, $df = 8$, $*P = 0.0114$.



(6), for 4 weeks. MEM-treatment significantly increased the number of DCX⁺ cells in the DG, indicating enhanced neurogenesis (fig. S8). We found significantly larger volumes of PSD95⁺Lamp1⁺ puncta within microglia in MEM-treated animals (Fig. 4, A and B). Additionally, MEM treatment facilitated forgetting after CFC training (Fig. 4, C and D), whereas

administering PLX blocked MEM-facilitated forgetting (Fig. 4D) without altering the enhanced neurogenesis by MEM (fig. S8).

To further investigate whether microglia also contribute to neurogenesis-unrelated forgetting, we used a GFAP-TK transgenic mouse line, which expresses herpes simplex virus thymidine kinase (TK) under the control of

the glial fibrillary acidic protein (GFAP) promoter. Administration of the antiviral drug ganciclovir (GCV) ablates only mitotic GFAP⁺ cells that express TK, thus depleting neurogenesis (29). To completely deplete integration of new neurons, we started treating TK^{+/-} mice and their wild-type littermates (TK^{-/-}) with GCV 4 weeks before CFC training and

continued until the test (Fig. 4E and fig. S9). PLX was administered after training to deplete microglia. GCV treatment in TK^{+/-} mice prevented forgetting, whereas TK^{+/-} mice treated with both PLX and GCV showed significantly higher levels of memory retention than TK^{+/-} mice treated with GCV only (Fig. 4F).

To confirm that microglia-mediated forgetting contributes to neurogenesis-unrelated forgetting, we injected AAV-DIO-CD55-mCherry or AAV-DIO-mCherry into c-Fos-Cre^{ERT2} mice to label engram cells in hippocampal CA1 (Fig. 4, G and H), which is not a neurogenic region. We found that expression of CD55 in CA1 engram cells also prevented forgetting (Fig. 4I) and dissociation of engram cells (Fig. 4, J and K).

Synaptic connections in the brain are highly dynamic and variable in strength and connectivity (14). Our study shows that microglia eliminate synaptic components in the adult hippocampus, whereas depleting microglia or inhibiting phagocytosis of microglia prevents forgetting. This suggests that synapse elimination by microglia leads to dissociation of engrams and the forgetting of previously learned contextual fear memory. In the developing brain, microglial engulfment of synapses depends on the classical complement cascade (15). Disruption of the microglia-specific phagocytic pathway by knocking out complement components, such as C1q, C3, or CR3, results in sustained deficits in synaptic connectivity (15, 24). C1q levels in the brain increase during aging, whereas C1q-deficient mice exhibit enhanced synaptic plasticity and less cognitive and memory decline when aged (30). Notably, our study showed that the C1q-dependent complement pathway is actively involved in synapse elimination by microglia in the healthy adult hippocampus. CD55 is a known inhibitor of complement pathways in the immune system and is expressed in neurons in response to chronic inflammation (31). We overexpressed CD55 to inhibit the complement pathways, specifically in engram cells, without affecting microglia or other neurons in the circuits, and we found that forgetting was prevented. This indicates that the elimination of synaptic structures by microglia in the DG of the healthy adult brain occurs in a complement-dependent manner. Moreover, inhibiting the activity of engram cells facilitates the forgetting of related memory, which could be blocked by depleting microglia or inhibiting complement pathways in

engram cells. This indicates that synapse elimination by microglia is also activity-dependent, following similar rules in the developing brain (15), thus resulting in the erasure of less-active memories. Besides eliminating synapses, microglia have also been reported to be able to trigger long-term synaptic depression via AMPA receptor internalization, through activation of CR3 (32), which may also contribute to forgetting.

New neurons are continuously generated in the DG, providing a substrate for massive synaptic reorganization and circuit rewiring in this region. Newborn dentate granule neurons integrate into hippocampal neural circuits by competitively replacing existing synaptic connections formed by mature granule neurons (7, 27), thus leading to the forgetting of hippocampal-dependent contextual fear memory (6). Our study shows that MEM-induced enhanced neurogenesis leads to increased synaptic engulfment by microglia, whereas depletion of microglia blocks facilitated memory forgetting induced by enhanced neurogenesis, suggesting that microglia contribute to neurogenesis-induced synaptic reorganization. Besides the rewiring of neural circuits caused by the continuous integration of newborn neurons, mature neurons are also able to reorganize their connectivity. We found that depletion of microglia in the DG without neurogenesis or inhibition of complement pathways in CA1 engram cells prevents forgetting. This indicates that microglia-mediated synaptic reorganization is also happening in mature hippocampal neurons, thus leading to weakening or loss of connections between engram cells and the forgetting of encoded memories. This also suggests that, in species lacking adult neurogenesis, or in non-neurogenic brain regions such as the cortex, microglia could be one major force contributing to synapse loss and forgetting.

REFERENCES AND NOTES

1. J. H. Han *et al.*, *Science* **316**, 457–460 (2007).
2. S. A. Josselyn, S. Köhler, P. W. Frankland, *Nat. Rev. Neurosci.* **16**, 521–534 (2015).
3. S. Tonegawa, M. Pignatelli, D. S. Roy, T. J. Ryan, *Curr. Opin. Neurobiol.* **35**, 101–109 (2015).
4. S. B. Hofer, T. D. Mrcic-Flogel, T. Bonhoeffer, M. Hübener, *Nature* **457**, 313–317 (2009).
5. G. Yang, F. Pan, W. B. Gan, *Nature* **462**, 920–924 (2009).
6. K. G. Akers *et al.*, *Science* **344**, 598–602 (2014).
7. N. Toni, A. F. Schinder, *Cold Spring Harb. Perspect. Biol.* **8**, a018903 (2015).
8. P. W. Frankland, S. Köhler, S. A. Josselyn, *Trends Neurosci.* **36**, 497–503 (2013).

9. M. Fu, Y. Zuo, *Trends Neurosci.* **34**, 177–187 (2011).
10. D. Tropea, A. K. Majewska, R. Garcia, M. Sur, *J. Neurosci.* **30**, 11086–11095 (2010).
11. J. T. Trachtenberg *et al.*, *Nature* **420**, 788–794 (2002).
12. J. E. Coleman *et al.*, *J. Neurosci.* **30**, 9670–9682 (2010).
13. A. Attardo, J. E. Fitzgerald, M. J. Schnitzer, *Nature* **523**, 592–596 (2015).
14. Y. Wu, L. Dissing-Olesen, B. A. MacVicar, B. Stevens, *Trends Immunol.* **36**, 605–613 (2015).
15. D. P. Schafer *et al.*, *Neuron* **74**, 691–705 (2012).
16. R. C. Paolicelli *et al.*, *Science* **333**, 1456–1458 (2011).
17. M. E. Tremblay, R. L. Lowery, A. K. Majewska, *PLoS Biol.* **8**, e1000527 (2010).
18. C. Madry *et al.*, *Neuron* **97**, 299–312.e6 (2018).
19. H. Wake, A. J. Moorhouse, S. Jinno, S. Kohsaka, J. Nabekura, *J. Neurosci.* **29**, 3974–3980 (2009).
20. M. Prinz, J. Priller, S. S. Sisodia, R. M. Ranshoff, *Nat. Neurosci.* **14**, 1227–1235 (2011).
21. R. A. Rice *et al.*, *J. Neurosci.* **35**, 9977–9989 (2015).
22. C. J. Guenther, K. Miyamichi, H. H. Yang, H. C. Heller, L. Luo, *Neuron* **78**, 773–784 (2013).
23. C. M. Sellgren *et al.*, *Nat. Neurosci.* **22**, 374–385 (2019).
24. B. Stevens *et al.*, *Cell* **131**, 1164–1178 (2007).
25. A. Nicholson-Weller, C. E. Wang, *J. Lab. Clin. Med.* **123**, 485–491 (1994).
26. M. M. Poo *et al.*, *BMC Biol.* **14**, 40 (2016).
27. N. Toni *et al.*, *Nat. Neurosci.* **10**, 727–734 (2007).
28. N. Toni *et al.*, *Nat. Neurosci.* **11**, 901–907 (2008).
29. J. S. Snyder, A. Soumier, M. Brewer, J. Pickel, H. A. Cameron, *Nature* **476**, 458–461 (2011).
30. A. H. Stephan *et al.*, *J. Neurosci.* **33**, 13460–13474 (2013).
31. J. van Beek *et al.*, *J. Immunol.* **174**, 2353–2365 (2005).
32. J. Zhang *et al.*, *Neuron* **82**, 195–207 (2014).

ACKNOWLEDGMENTS

We thank all the members of the Y.G. and La.W. laboratories for the discussion and constructive suggestions for this project. We thank P. Frankland for his critical comments. We are grateful to the Core Facilities of Zhejiang University School of Medicine for technical assistance. **Funding:** This work was supported by grants from the National Key R&D Program of China (2017YFA0104200), the Zhejiang Provincial Natural Science Foundation of China (LR17C090001) to Y.G., the National Natural Science Foundation of China (31700888) to La.W., and the Natural Science Foundation of Zhejiang Province (LZ19C090001) to B.S. **Author contributions:** C.W., H.Y., La.W., and Y.G. designed all of the experiments; C.W. performed all behavior tests, imaging, and most of the analysis; H.Y. performed vector constructions, viral injections, and some imaging; Z.H. and Y.S. performed some image analysis; J.M. and J.L. helped in genotyping some animals; X.-D.W. provided c-Fos-Cre^{ERT2} and hM4Di mice; Li.W. provided Ai14 mice; B.S. provided GFAP-TK mice; P.S. provided CX3CR1^{GFP/+} and CD11b-DTR mice; C.W., H.Y., La.W., and Y.G. discussed the results and wrote the manuscript; and all authors discussed the manuscript. **Competing interests:** The authors declare no competing interests. **Data and materials availability:** All data needed to understand and assess the conclusions of this study are included in the text, figures, and the supplementary materials.

SUPPLEMENTARY MATERIALS

science.sciencemag.org/content/367/6478/688/suppl/DC1
Materials and Methods
Figs. S1 to S9
References (33, 34)
Movies S1 to S5

[View/request a protocol for this paper from Bio-protocol.](#)

27 August 2019; accepted 6 January 2020
10.1126/science.aaz2288

Microglia mediate forgetting via complement-dependent synaptic elimination

Chao Wang, Huimin Yue, Zhechun Hu, Yuwen Shen, Jiao Ma, Jie Li, Xiao-Dong Wang, Liang Wang, Binggui Sun, Peng Shi, Lang Wang and Yan Gu

Science **367** (6478), 688-694.
DOI: 10.1126/science.aaz2288

Microglia modulate memories

Synaptic reorganization and circuit rewiring leads to loss or weakening of connections between neurons and may result in the erasure of previously formed memories. Microglia eliminate excessive synapses in the developing brain and regulate the dynamics of synaptic connections between neurons throughout life. However, it is still unclear whether forgetting is related to microglia activity and how microglia regulate memory erasure in the adult brain. Wang *et al.* discovered that microglia eliminated synaptic components in the adult hippocampus and that depleting microglia or inhibiting phagocytosis of microglia prevented forgetting. Synapse elimination by microglia may thus lead to degradation of memory engrams and forgetting of previously learned contextual fear memory.

Science, this issue p. 688

ARTICLE TOOLS

<http://science.sciencemag.org/content/367/6478/688>

SUPPLEMENTARY MATERIALS

<http://science.sciencemag.org/content/suppl/2020/02/05/367.6478.688.DC1>

RELATED CONTENT

<http://stm.sciencemag.org/content/scitransmed/9/421/eaai7635.full>

REFERENCES

This article cites 34 articles, 10 of which you can access for free
<http://science.sciencemag.org/content/367/6478/688#BIBL>

PERMISSIONS

<http://www.sciencemag.org/help/reprints-and-permissions>

Use of this article is subject to the [Terms of Service](#)

Science (print ISSN 0036-8075; online ISSN 1095-9203) is published by the American Association for the Advancement of Science, 1200 New York Avenue NW, Washington, DC 20005. The title *Science* is a registered trademark of AAAS.

Copyright © 2020 The Authors, some rights reserved; exclusive licensee American Association for the Advancement of Science. No claim to original U.S. Government Works